Clays and Clay Minerals, Vol. 36, No. 3, 233–242, 1988.

MODIFICATION OF THE POROUS STRUCTURE AND SURFACE AREA OF SEPIOLITE UNDER VACUUM THERMAL TREATMENT

Y. GRILLET,[1] J. M. CASES,[2] M. FRANCOIS,[2] J. ROUQUEROL,[1] AND J. E. POIRIER[2]

[1] Centre de Thermodynamique et de Microcalorimétrie du C.N.R.S.
26, rue du 141ème RIA, 13003 Marseille, France

[2] Centre de Recherche sur la Valorisation des Minérais
et U.A. 235 "Minéralurgie," B.P. 40, 54501 Vandoeuvre Cédex, France

Abstract—Modifications of the external surface area and the two types of microporosity of sepiolite (structural microporosity and inter-fiber porosity) were examined as a function of the temperature of a vacuum thermal treatment to 500°C. The methods used included: reciprocal thermal analysis, N_2 and Ar low-temperature adsorption microcalorimetry, gas adsorption volumetry (for N_2, Ar, and Kr at 77 K and CO_2 at 273 and 293 K), water-vapor adsorption gravimetry, and immersion microcalorimetry into liquid water at 303 K. If the sample was not heated >100°C, only 20% of the structural microporosity was available to N_2, whereas 52% was available to CO_2 at 293 K. In both experiments, the channels filled at very low relative pressures. At >350°C, the structure transformed to anhydrous sepiolite, which showed no structural microporosity. The inter-fiber microporosity decreased from 0.031 to 0.025 cm^3/g (as seen with N_2), and the external specific surface area decreased from 120 to 48 m^2/g. The water adsorption isotherms showed a lower and lower affinity of the external surface of fibers for water as the temperature of thermal treatment increased. The thickness of the bound water on the external surface was estimated to be ≤3.5 monolayers, i.e., less than 10 Å.

Key Words—Adsorption microcalorimetry, Microporosity, Reciprocal thermal analysis, Sepiolite, Surface area, Thermal treatment.

INTRODUCTION

Sepiolite is a fibrous magnesian silicate having a formula that may be written as $Si_{12}Mg_8O_{32}\cdot nH_2O$. Its structure was first determined by Nagy and Bradley (1955), and then, more accurately, by Brauner and Preisinger (1956) and Brindley (1959) who used X-ray powder diffraction data, and finally by Rautureau and Tchoubar (1976) who used selected-area electron diffraction data. These studies have shown that sepiolite is made up of talc-like layers arranged in long ribbons stuck together to form the fibers. A cross section, as seen by the "lattice imaging" technique, shows numerous {110} faces in which the talc-like ribbons are arranged in staggered rows separated by channels parallel to the fiber axis. These channels are referred to as structural micropores (size = 13.4 × 6.7 Å). Larger pores, having diameters of 20–200 Å, are also present between fibers (Rautureau and Tchoubar, 1976; Rautureau and Mifsud, 1977).

Thermogravimetric analysis at <200°C shows an initial weight loss of about 12%, corresponding to zeolitic water contained in the channels. A further weight loss of about 6% between 200° and 600°C may be attributed to the removal of the water bonded to Mg^{2+} on the edges of the talc ribbons. A final weight loss of about 3% at >650°C corresponds to the dehydroxylation of the mineral (Prost, 1975). The zeolitic water mentioned above may also be removed by simple outgassing at room temperature. Concurrent with the second dehydration at >350°C, sepiolite transforms into "anhydrous sepiolite" (Preisinger, 1963), in which the talc-like layers are tilted with respect to each other.

Fibrous clay minerals have numerous industrial (Barrer *et al.*, 1959) and pharmaceutical applications, mainly due to their high surface area and to their structural channels. Actually, the location of the "micropores" (Sing *et al.*, 1985) responsible for sepiolite's adsorption capacity is somewhat controversial. Barrer and Mackenzie (1954) and Dandy (1968, 1971) suggested that the availability of these structural channels to the nitrogen molecules is limited. The loss in BET-N_2 surface area observed on outgassing at >200°C has been attributed to a sintering of the external fiber surface (Dandy and Nadiye-Tabbiruka, 1975). On the other hand, Moller and Kolterman (1965), Delon and Cases (1970), Fernandez Alvarez (1970, 1978), and Jimenez-Lopez *et al.* (1978) suggested that the nitrogen molecule may easily enter the structural channels after the zeolitic water is removed.

Most of the studies quoted above were based upon adsorption isotherms which reveal no information about relative pressures <0.07. Hence, the usual method to detect and study microporosity (Lippens and de Boer, 1965; Sing, 1967) could not be applied to reveal various types of microporosity of sepiolite (Dubinin, 1966).

Our approach to understand better the microporous structure of sepiolite is based on a well-controlled thermal treatment and outgassing procedure and makes use of nitrogen- or argon-adsorption microcalorimetry (at 77 K), which yields information in the low-pressure range, and of immersion microcalorimetry in water, which allows surface area to be determined by the so-called "absolute" method of Harkins and Jura (1944).

EXPERIMENTAL

Materials

The sepiolite studied here was from Vallecas, Spain, and was supplied by Tolsa S.A. It is a defibrated sepiolite (trade name, Pangel) obtained by wet-process micronization. Its mineralogical purity was >95%, and the equivalent spherical diameter of all particles was <10 μm.

Reciprocal thermal analysis

In conventional thermal analysis a physical property of a substance is measured as a function of temperature. The substance is subjected to a controlled temperature program, which is nearly always linear with time. For clay minerals, this type of procedure usually results in a partial overlap of successive dehydration or outgassing steps. In the present study this problem was overcome by applying reciprocal thermal analysis (RTA), also called controlled- (or constant-) transformation-rate thermal analysis (Rouquerol, 1970, 1987). In this process the rate of dehydration or outgassing is kept constant (or controlled) over the entire temperature range of the experiment by means of an appropriate heating control loop, which results in an *a priori* unknown temperature program. The system operates in the reverse way of conventional thermal analysis because the temperature is measured while a temperature-dependent property of the substance (here, the water content) is modified at a constant (or controlled) rate. In RTA, the rate of dehydration of the clay may be controlled at any value low enough to ensure a satisfactory elimination of the temperature and pressure gradients within the sample, i.e., to ensure a satisfactory separation of the successive steps of the dehydration. The simplest assembly is that of Rouquerol (1970), in which the flow of gas evolved from the sample submitted to a dynamic vacuum is used to control the heating of the furnace. For a constant composition of the gas evolved (here, water vapor), the temperature vs. time data may be immediately converted into temperature vs. mass-loss data (inasmuch as the rate of dehydration is constant), and therefore to a conventional thermogravimetric curve. The experimental conditions selected in the present study were a sample mass of about 0.5 g, a residual pressure of 4 mtorr over the sample, and a dehydration rate of 1.24 mg/hr.

Gas-adsorption microcalorimetry at 77 K

Gas-adsorption microcalorimetry (Rouquerol, 1972) allows a simultaneous recording of the adsorption isotherm of nitrogen or argon and the corresponding derivative enthalpy. For that purpose, the adsorbable gas is introduced into the adsorption cell at a slow and constant flow rate under quasi-equilibrium conditions. The adsorption cell is surrounded by an isothermal microcalorimeter kept at 77 K by total immersion in a liquid nitrogen bath. The microcalorimeter makes use of two heat-flow Tian-Calvet thermopiles (1000 thermocouples each, around a cylindrical cell of 50 cm^3) connected in a differential assembly.

Both the quasi-equilibrium pressure (by means of a diaphragm pressure transducer which, for these experiments, is of the Barocel Datametrics capacitance type) and the heat flow due to the adsorption phenomenon may then be recorded as a function of time. A computer program derives the adsorption isotherm, the content of a monolayer (as calculated from the BET equation), and the derivative (or "differential") enthalpy of adsorption vs. coverage (the latter being taken equal to 1, for the completion of the monolayer).

Prior to each experiment, 150-mg samples were outgassed under the conditions of RTA given above up to final temperatures of 25°, 100°, 200°, 250°, 350°, or 500°C.

Adsorption gravimetry of water vapor

The experimental apparatus (Rouquerol and Davy, 1978) was built around a Setaram MTB 10-8 symmetrical microbalance. A 60-mg sample was outgassed under vacuum from 25° to 500°C. Water vapor was supplied from a source kept at 41°C, here again at a slow flow-rate (through a Granville-Philips leak valve) to ensure quasi-equilibrium conditions at all times. The adsorption isotherm (here, mass adsorbed at 303 K vs. quasi-equilibrium pressure) was directly recorded on a simple X-Y recorder.

Immersion microcalorimetry in water

Immersion microcalorimetry was used to determine the enthalpy of immersion in water of sepiolite samples vs. the pre-equilibration P/P_0 relative pressure of water vapor. This enthalpy curve was then used to derive the external (i.e., non-microporous) surface area by applying a modified Harkins and Jura method (Partyka *et al.*, 1979; Cases and François, 1982; Fripiat *et al.*, 1982).

For that purpose, a glass bulb (with brittle end) containing about 90 mg of sepiolite was successively outgassed, pre-equilibrated with vapor pressure at the desired conditions, sealed, and then introduced into the experimental cell (half-filled with water) of a conventional Tian-Calvet microcalorimeter (Setaram, 100-cm^3 cells). About 3 hr was needed for a satisfactory thermal equilibrium (i.e., to ensure that in any point of the

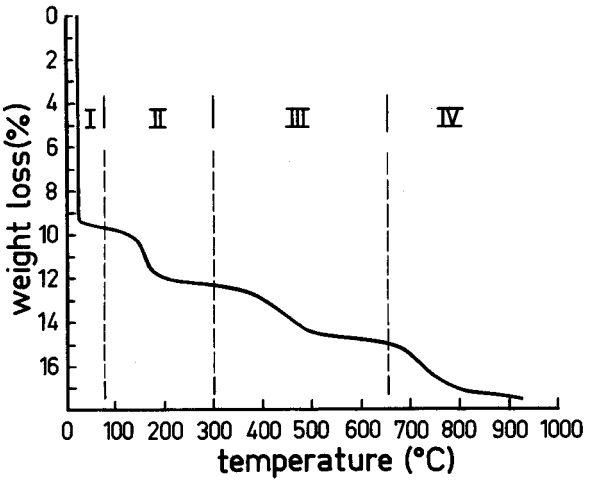

Figure 1. Reciprocal thermal analysis of Vallecas sepiolite.

calorimetric assembly the temperature was constant within 10^{-5} K). The brittle end was then broken by depressing a glass rod to which the bulb was attached. The immersion liquid entered the bulb and wet the sample, and the resulting heat flow was recorded as a function of time. The total heat effect was determined by integrating the curve, whereas the corrections due to the heat of vaporization of water in the void volume of the bulb and to the heat of breaking of the bulb were taken into account to derive an enthalpy of immersion dependent only on the sample and temperature and not on the calorimetric apparatus or procedure. The experiment at 303 K was repeated for increasing values of the pre-equilibration pressure.

Nitrogen-, krypton-, and CO_2-adsorption volumetry

For checking purposes, a few BET surface areas were determined by nitrogen or krypton adsorption, using a conventional BET volumetric equipment. Similar equipment was also used to study the microporosity of the samples by CO_2 adsorption volumetry at 273 and 293 K and by nitrogen adsorption at 77 K, using a method described elsewhere (Guérin *et al.*, 1970).

RESULTS

Figure 1 shows the reciprocal evolved-gas-detection thermal analysis curve for the sepiolite sample. The successive dehydration steps previously shown by thermogravimetric analysis (TGA) (Rautureau and Tchoubar, 1976) are clearly evident. Region I, between room temperature and 75°C, corresponds to the evolution of the zeolitic water proper (9.7% of the initial sample mass). The next two regions correspond to the expulsion of water bound to the Mg atoms on the edges of the sheet: half (i.e., 2.7% of the initial sample mass) was lost in region II (70°–300°C), and the other 2.7% was lost in region III (300°–650°C). The final 2.4% lost in region IV (>650°C) was due to dehydroxylation of

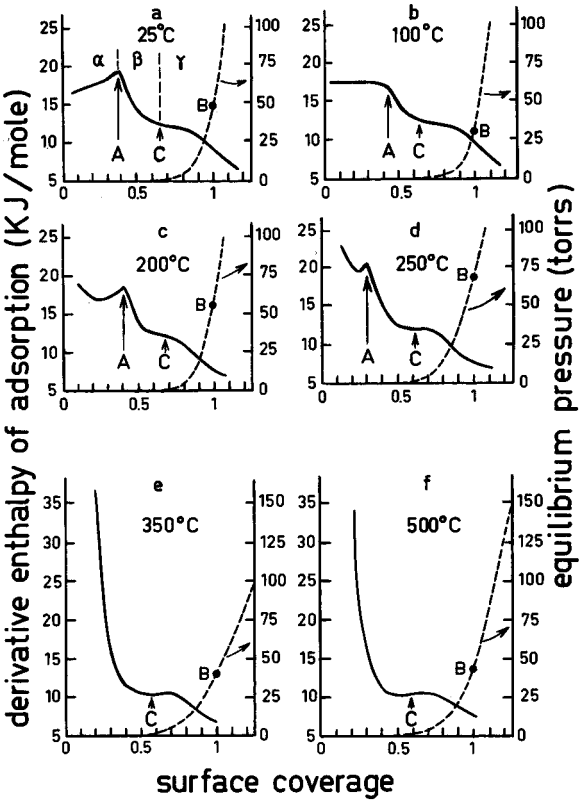

Figure 2. Derivative enthalpy of adsorption (solid line) and equilibrium pressure (dashed line) vs. coverage for the sepiolite-nitrogen systems at 77 K.

the mineral. The total loss was in accord with Brauner and Preisinger's model. The temperatures corresponding to the highest reaction rates were 25°C for region I, 154°C for region II, 428°C for region III, and 725°C for region IV.

The curves representing the derivative enthalpy of adsorption of nitrogen vs. coverage, at 77 K, on a series of six samples brought to different extents of outgassing are shown in Figure 2. The corresponding adsorption isotherms are shown in the same illustration, but not in the conventional way. Inasmuch as coverage is already included in the abscissa (for the presentation of the enthalpy data), the equilibrium pressure is used as the ordinate. Coverage was calculated by assuming it to be unity at point B of the adsorption isotherm (Emmett and Brunauer, 1937). This point is close, but slightly less than, the point at which the enthalpy of adsorption merges into the enthalpy of liquefaction. This information, which will clarify in the discussion of these complex enthalpy curves, is practically unavailable by the isosteric method, which lacks accuracy in the low-pressure range involved and which is based on the assumption—here unlikely—of an exactly similar state of the adsorbed phase at the two temperatures of observation needed by the method. A similar set of

https://doi.org/10.1346/CCMN.1988.0360304 Published online by Cambridge University Press

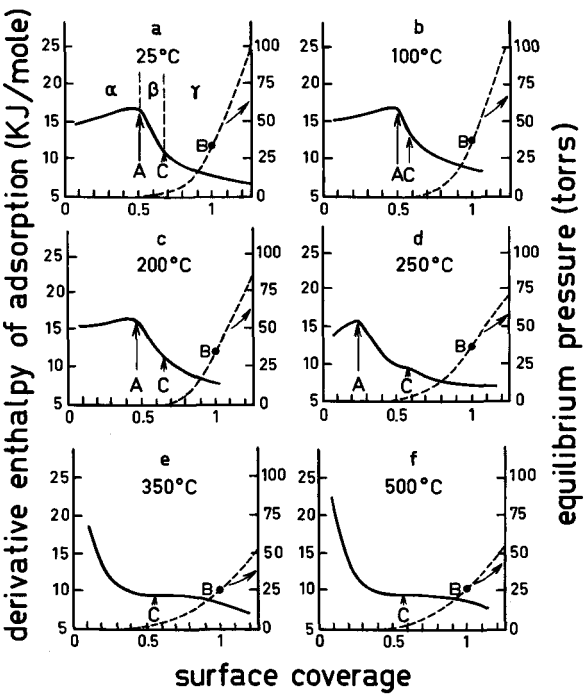

Figure 3. Derivative enthalpy of adsorption (solid line) and equilibrium (dashed line) vs. coverage for the sepiolite-argon systems at 77 K.

curves (derivative enthalpy and corresponding adsorption isotherm) obtained for argon, also at 77 K, is given in Figure 3.

The adsorption isotherms given in Figures 2 and 3 were re-plotted following the procedure of de Boer *et al.* (1966) in the form V_a vs. t, where t is the mean thickness of the adsorbed layer, which is known from a "universal" reference curve obtained with the same adsorbate but with a non-microporous adsorbent. Any non-microporous solid normally yields a linear "t-plot" (i.e., V_a vs. t) passing through the origin. Its slope is proportional to the specific surface area of the solid examined. On the other hand, microporous solids yield a non-linear "t-plot" corresponding to the filling of the micropores (large uptake and steep slope) followed by adsorption on the non-microporous parts of the surface (generally smaller uptake and always less steep slope), which may be called the "external" surface, S_{ext}. The latter part of the t-plot is commonly linear. Its slope yields a value of S_{ext}, whereas its intercept with the V_a axis allows the microporous volume to be derived, after converting V_a into a liquid volume V_0 (liq), which is given, together with S_{ext}, in Table 1. The t curve was chosen to have the same energetic constant C value (C ~270) as the system under consideration in order to ensure that S_{total} was equal to S_{BET} (Mikhail *et al.*, 1968).

The equivalent specific surface area of the sample outgassed at ≤100°C was determined in various ways: (a) by using the BET method (point by point volumetry at 77 K) either with nitrogen (324 m^2/g with a cross-sectional molecular area of 0.163 nm^2) or with krypton (314 m^2/g with a molecular area of 0.143 nm^2), or (2) by using the "point B" method (318 m^2/g) on the low-temperature adsorption calorimetry data (cf. Figure 6).

CO_2 adsorption at 273 and 293 K was used to study the changes in microporosity during outgassing. Dubinin's equation (1966) was applied:

$$\log V = \log V_0 - D(\log[P/P_0])^2,$$

where V is the volume of gas adsorbed; V_0 is the volume of gas which, once adsorbed, is able to fill completely the micropores; and P_0 is the saturating vapour pressure (here, 3,485,565 Pa at 273 K and 5,727,809 Pa at 293 K). V_0 may be converted into a liquid volume

Table 1. Equivalent specific surface areas and micropore volumes of sepiolite.

Final outgassing temperature (°C)	N_2 adsorption at 77 K t plot			Low-temperature adsorption calorimetry	CO_2 adsorption			H_2O adsorption at 303 K		
	V_0 liq (cm^3/g) 1	S total (m^2/g) 2	S ext (m^2/g) 3	$S_{\beta+\gamma}$ (m^2/g) 4	T (K)	V_0 liq (cm^3/g) 5	S (m^2/g) 6	V_m liq (cm^3/g) 7	S (m^2/g) 8	C 9
25	0.040	364	240	211				0.0655	324	44
100	0.046	340	195	183	273 293	0.1091 0.1293	294 345	0.0649	321	29
200	0.034	321	222	193	273 293	0.0208 0.0208	56 55	0.0672	332	5, 6
250	0	196			273 293	0.0233 0.0196	63 52	0.0402	199	3, 8
350	no linear relationship				273 293	0.0194 0.0179	52 48	0.0237	117	5, 2
500	0	120						0.0264	131	2, 8

1, 5 = Total micropore volume per unit mass of adsorbent as calculated with the liquid adsorptive. 2, 6, 8 = Total specific surface area. 3 = External specific surface area. 7 = Monolayer capacity calculated from the BET equation per unit mass of adsorbent as calculated with density of the liquid adsorptive. 4 = Equivalent surface area of structural and inter-fiber microporosity. 9 = Energetic constant of BET theory.

https://doi.org/10.1346/CCMN.1988.0360304 Published online by Cambridge University Press

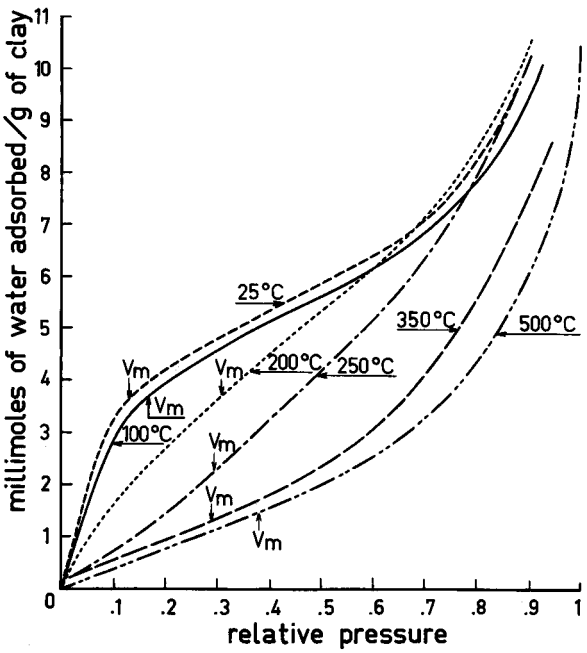

Figure 4. Influence of outgassing temperature on adsorption isotherms of water on sepiolite at 303 K.

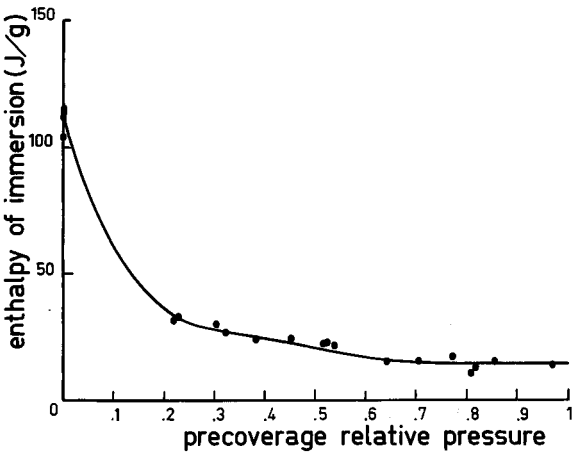

Figure 5. Enthalpy of immersion vs. precoverage relative pressure for the sepiolite-water systems at 303 K.

V_0 (liq) (using a density of 1.08 and 1.05 g/cm^3 for liquid CO_2 at 273 and 293 K, respectively; Anonymous, 1976) as reported in Table 1, column 7. An equivalent specific surface area may also be derived from V_0, taking a cross-sectional molecular area of 0.182 and 0.185 nm^2 at 273 and 293 K, respectively (cf. Table 1, column 8 and also Figure 6) (Guérin *et al.*, 1970).

The adsorption isotherms of water at 303 K on the differently outgassed sepiolite samples are given in Figure 4. The location of the monolayer as calculated by the BET method is indicated on each isotherm by V_m. The exact value of V_m (the *liquid* volume (cm^3/g) of water corresponding to the monolayer) is given in Table 1, column 9. The corresponding value of the BET energetical constant C (column 11) and of the equivalent surface area (calculated with a molecular area of 0.148 nm^2 (Hagymassy *et al.*, 1969) (column 10 and Figure 6) are also given.

The enthalpy of immersion of sepiolite in water, after a common outgassing at 105°C for 5 hr, but for increasing precoverage relative pressures, is given in Figure 5. The enthalpy drops to an approximately constant value for relative pressures >0.7. This value was used to derive the specific surface area, following the Harkins and Jura method, using a value of 119.5 mJ/m^2 for the internal energy of the water surface at 303 K (Cases and François, 1982). The result was 125 m^2/g.

DISCUSSION

Interpretation of the adsorption enthalpy data

As shown in Figures 2 (nitrogen adsorption) and 3 (argon adsorption) for samples outgassed at ≤250°C, three main ranges (given by the letters α, β, and γ in Figures 2a and 3a) may be separated:

1. Range α extends to point A on the curves. For argon in this range the derivative enthalpy of adsorption, $\Delta_{ads}\dot{h}$, steadily increases with adsorption. The same was observed for adsorption on homogeneous surfaces (e.g., those of graphite or molecular sieves) in which the energetic interaction between adsorbed molecules increases simultaneously over all the adsorbed phase. These observations mean that there is no screening effect due to surface heterogeneities which would give rise to a decrease of $\Delta_{ads}\dot{h}$ vs. coverage. This range appears to correspond to the filling of the structural micropores. The more complicated shape of the nitrogen adsorption curve in the same coverage range may be explained by the quadrupole moment and the smaller size (in one direction) of the nitrogen molecule whose dimensions are 3 and 4.1 Å (Pauling, 1940), as compared with 3.83 Å for the argon molecule. Under these conditions, the nitrogen molecule is more sensitive to surface heterogeneities, which are progressively made available during outgassing and which give rise to an initial decrease in $\Delta_{ads}\dot{h}$ vs. coverage. For the sample outgassed at 100°C, this decrease completely cancelled the increase observed for the sample outgassed at 25°C. In contrast, both phenomena were clearly superimposed for the samples outgassed at 200° or 250°C. The α domain disappeared when the samples were outgassed at ≥350°C because the silicate layers became tilted and the structural microporosity vanished.

2. Range β extends between points B and C; here, a drop of $\Delta_{ads}\dot{h}$ vs. coverage was observed. Point C is in most cases an inflection point (Figures 2a, 2b, 3e, and 3f) or a point where the slope changes (Figures 2d–2f), whereas, as in Figures 3a–3c, the point C abscissa is the intersection of the straight lines extrapolated from the straight part of range β and from the end of range γ. Range β probably corresponds to the filling of wider

https://doi.org/10.1346/CCMN.1988.0360304 Published online by Cambridge University Press

Table 2. Low-temperature adsorption calorimetry results for sepiolite.

Final outgassing temperature (°C)	Range	N_2 adsorption at 77 K				Ar adsorption at 77 K				$(V_B)Ar$ / $(V_B)N_2$
		S_{total} (m^2/g) 1	V_B liq (cm^3/g) 2	V_i (cm^3/g) 3	S_{ext} (m^3/g) 4	S_{total} (m^2/g)	V_B liq (cm^3/g)	V_i (cm^3/g)	S_{ext} (m^3/g)	
25		351	0.1248		123	332	0.1120		108	0.90
	α			0.0499				0.0560		
	β			0.0312				0.0197		
	total			0.0811				0.0757		
100		318	0.1130		119	311	0.1049		131	0.87
	α			0.0480				0.0525		
	β			0.0226				0.0083		
	total			0.0706				0.0608		
200		325	0.1156		106	307	0.1034		108	0.90
	α			0.0474				0.0491		
	β			0.0306				0.0181		
	total			0.0780				0.0672		
250		190	0.0676		76	182	0.0614		91	0.89
	α			0.0187				0.0138		
	β			0.0226				0.0169		
	total			0.0413				0.0307		
350		129	0.0460		55	122	0.0411		55	0.90
	β			0.0265				0.0226		
500		119	0.0423		48	113	0.0381		48	0.90
	β			0.0254				0.0219		

1 = Total specific surface area. 2 = Monolayer capacity obtained from the point B per unit mass of adsorbent as calculated with density of the liquid adsorptive. 3 = Micropore volume per unit mass of adsorbent as calculated with density of the liquid adsorptive. 4 = External specific surface area.

micropores than those filled in range α, although the range persisted at very low pressures. As seen in Figures 2 and 3, point C was always reached for relative pressures <0.007 (out of range of most pressure gages used in this type of study). The latter micropores may be due either to inter-fiber microporosity or to defects in the arrangement of the structural units (Rautureau and Tchoubar, 1976), and the wide range of $\Delta_{ads}\dot{h}$ suggests a wide range in micropore size.

3. Range γ extends beyond point C, where the monolayer was progressively built up on the external surface of fibers as the equilibrium pressure increased appreciably. The difference in $\Delta_{ads}\dot{h}$ between the nitrogen and the argon experiments allows the determination of the "specific" interaction of the nitrogen molecule with this surface, due to its quadrupole momentum, which is 2–3 kJ/mole.

The amounts of either nitrogen or argon adsorbed in ranges α and β may be converted into liquid volumes using the values 0.808 and 1.427 for the specific gravity at 77 K of liquid nitrogen and liquid argon, respectively, as reported in Table 2, column 5. Moreover, the liquid volume V_B corresponding to the amount adsorbed at "point B" (as defined by Emmett and Brunauer, 1937) may also be calculated, and an "equivalent" specific surface area, S, may be derived, taking into account a cross-sectional area of 0.162 and 0.138 nm^2 for the nitrogen and argon molecules, respectively (McClellan and Harnsberger, 1967), as also shown in Table 2. The word "equivalent" is, of course, used here to point out the partial inadequacy of the above calculation for a microporous solid in which the adsorbed molecule does not cover at all the same area as on a flat surface (Sing *et al.*, 1985). Finally, the amount adsorbed in range γ to point B yields information on the external surface area of the fibers, S_{ext}, as is also given in Table 2.

These hypotheses on the physical meaning of the α, β, and γ domains can be confirmed by the following ways:

1. Calculation of the external area of fibers. For the sample outgassed at <100°C, the external area of fibers may be determined by three procedures. The first procedure relies on the enthalpy of immersion (Harkins and Jura "absolute" method) and yields a value of 125 m^2/g (Figure 6). The second procedure makes use of the statistical measurement by electron microscopy of the mean thickness of the elementary fiber, which is close to 160 Å. Assuming a square cross section leads to a surface area of about 120 m^2/g. The third procedure uses a detailed analysis of the water-adsorption isotherms at 303 K at relative pressures of <0.15. Three ranges may be distinguished (cf. Figure 7); the upper one (for $0.06 < P/P_0 < 0.13$) probably corresponds to the filling of a monolayer on the external surface. The amount adsorbed over range III leads to an external specific surface area of about 115 m^2/g.

https://doi.org/10.1346/CCMN.1988.0360304 Published online by Cambridge University Press

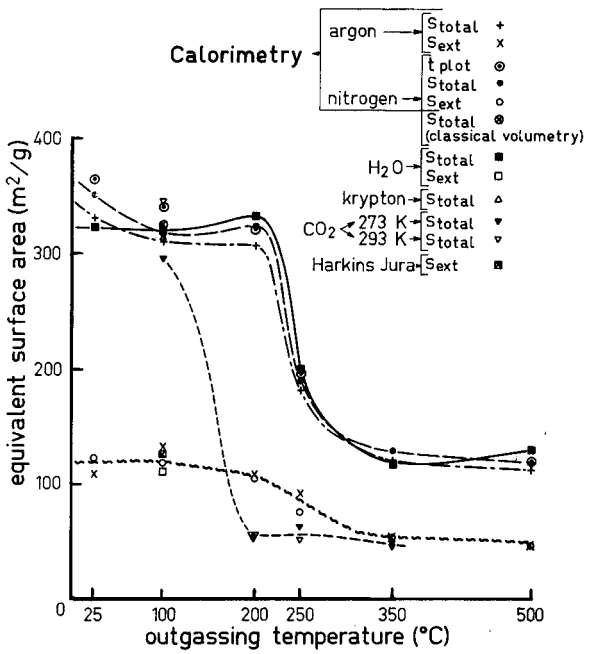

Figure 6. Effect of heat treatment on the equivalent specific surface area and external surface area of sepiolite obtained with different adsorbates and methods.

Thus, the recognition of three adsorption ranges, which were made first simply on the basis of the nitrogen- (or argon-) adsorption enthalpy curves (cf. Figures 2 and 3), has been supported by independent determinations. Indeed, the external surface areas which were derived from the amount adsorbed over range γ (to point B) (cf. Table 2) are 123 and 119 m^2/g (N_2 adsorption on samples outgassed below 25°C or 100°C, respectively) or 108 and 131 m^2/g (Ar adsorption on the same samples), which compare well with the values calculated above. The arithmetical mean of all the above values is 120 m^2/g, and may be taken as the external specific surface area of the sepiolite samples outgassed at $\leq$100°C.

2. Evaluation of structural microporosity. It is worthwhile to compare the thermal analysis curve (Figure 1) with the different specific surface areas of the sepiolite (Figure 6), either "total equivalent" (cf. upper curves) or "external" (cf. lower curve). In range II the thermal analysis curve is similar to the curve of total-equivalent specific surface area available to CO_2. Indeed, at the beginning of range II, this area amounts to about 300 m^2/g and decreases to about 55 m^2/g as the sample loses water (steep-break in the middle of range II of the thermal analysis curve, Figure 1) by outgassing at $\leq$200°C. This water corresponds to half the water initially bound to the Mg ions located on the edge of the talc ribbons. Apparently the resulting structure change is such that the initial microporosity (i.e., the microporosity formed by the staggered arrangement of the talc ribbons making up the fibers) is no longer available to the CO_2 molecule. A similar decrease in surface area (Figure 6) was shown by the other adsorbates (argon, nitrogen, water), but only after outgassing at a somewhat higher temperature (at least 300°C instead of 200°C). These data suggest that, although almost no water was evacuated between 200° and 300°C (Figure 1), the structure of the fibers changed progressively such that, after the silicate layers were tilted, their internal micropores became unavailable even to the water molecule.

The microporous volumes calculated (Table 1) from de Boer's t-plot (1966) (0.040 cm^3/g after outgassing at 25°C and 0.046 cm^3/g after outgassing at 100°C), are relatively close to those calculated from the adsorption enthalpy data and which correspond to adsorption range α (Table 2). For example, the micropore volumes for nitrogen was 0.049 and 0.048 cm^3/g for the outgassing temperatures listed above. Nevertheless, they are considerably smaller than those calculated from CO_2 adsorption (0.11 cm^3/g at 273 K and 0.13 cm^3/g at 293 K) or from the theoretical dimensions of the channels (0.2478 cm^3/g, Rautureau and Tchoubar, 1976) or from the other literature sources (0.1700 cm^3/g, Fernandez Alvarez, 1978; 0.1366 cm^3/g, Delon and Cases, 1970).

3. Evaluation of inter-fiber microporosity. As mentioned above, adsorption range β (Figures 2 and 3) is probably due to filling of inter-fiber micropores and of structural defects. This hypothesis is supported by the fact that the external surface calculated from the t-plot (Table 1, column 4) contains in fact both the external surface of the fiber and the surface due to inter-fiber microporosity. The values obtained are close to that calculated from low-temperature gas-adsorption microcalorimetry, taking into account only the extension of β and γ domains (Table 1, column 5).

The volume of these micropores available to nitrogen decreased from 0.031 to 0.025 cm^3/g when the final outgassing temperature was increased from 25°C to 500°C. At the same time, the sticking (or sintering) of the fibers appreciably reduced the external surface of fibers (from 120 to 48 m^2/g; cf. Table 2 and Figure 6).

Provisional conclusions

From the above considerations, depending on the method used, the starting structural microporosity appears to be 0.050 cm^3/g (N_2 or Ar adsorption) or 0.13 cm^3/g (CO_2 adsorption), i.e., 20 to 52% of the theoretical microporosity, as calculated from the structural parameters (Rautureau and Tchoubar, 1976). The inter-fiber microporosity of the commercial sepiolite sample (which had undergone an appropriate treatment) is about 0.030 cm^3/g.

The distance at which the surface still has an energetical effect on water adsorption, i.e., the thickness of the layer in energetical interaction with the surface (Fri-

https://doi.org/10.1346/CCMN.1988.0360304 Published online by Cambridge University Press

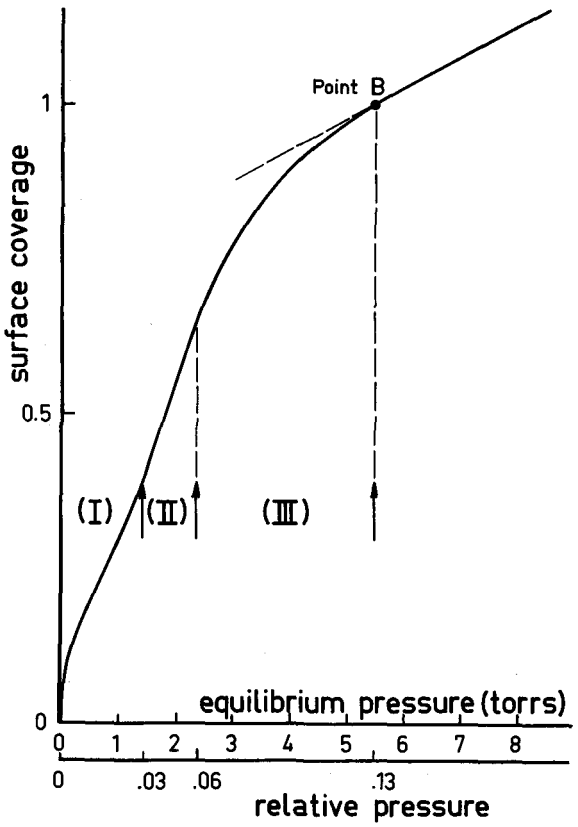

Figure 7. Adsorption isotherm for the sepiolite-water systems at 303 K and low relative pressures: outgassing temperature = 100°C.

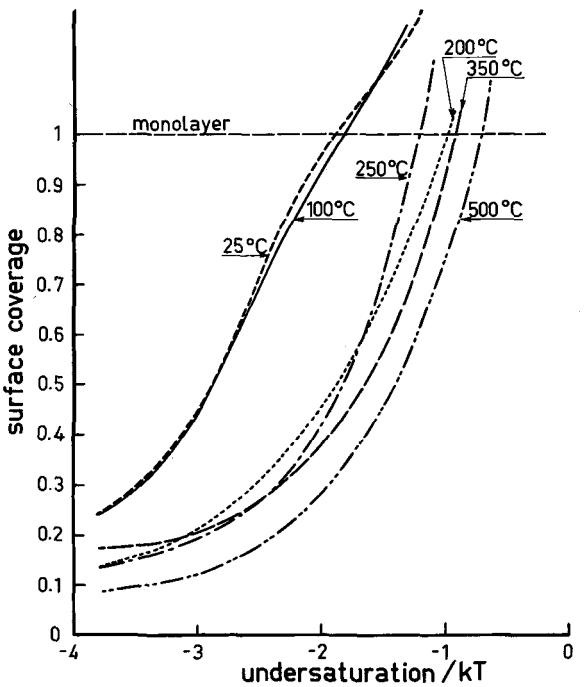

Figure 8. Adsorption isotherms for the sepiolite-water systems at 303 K in the plane (θ, ln P/Po).

piat *et al.*, 1982), may also be estimated on the basis of the enthalpies of immersion in water for several increasing precoverage pressures (Figure 5). The enthalpy of immersion remained unchanged for precoverage relative pressures of >0.7, which means that the thickness of the adsorbed layer was enough to screen completely the energetical effect of the surface. From the water adsorption isotherm on the same sample outgassed at ≤ 100°C, the amount adsorbed between relative pressures 0.06 and 0.7 (and therefore supposed to be adsorbed on the external surface of the fibers, cf. Figure 7) may be determined and, hence, the number of water monolayers adsorbed on the external surface of the fibers can be calculated provided its area (120 m^2/g) and the cross-sectional area of a water molecule (0.148 nm^2). The corresponding number of monolayers is 3.5. The actual number is probably smaller because a higher density (cross-sectional area of a water molecule, 0.106 nm^2) may be expected for the second and third layers of the bound water because the state of water molecule is closer to that of the liquid state than to that of the structured first layer. In this condition the lowest value would be 2.5.

The maximum volume of water in energetical interaction with the surface may then involve: (1) the external layer (0.085 cm^3/g, from the adsorption isotherm); (2) the inter-fiber microporosity (0.030 cm^3/g); and (3) the structural microporosity (at most, 0.248 cm^3/g, Rautureau and Tchoubar, 1976). The total volume (0.363 cm^3/g) is similar to that estimated by Fripiat *et al.* (1984) from nuclear magnetic resonance determination of deuteron relaxation time (0.480 cm^3/g).

In Figure 8, the water adsorption isotherms are plotted in the form θ (where $\theta = n_a/n_m$) vs. ln (P/P_0), where n_a represents the number of molecules adsorbed and n_m the monolayer capacity. Under any give conditions, the value of ln (P/P_0) at which the adsorption takes place is directly related to the strength of the "normal" adsorbate adsorbent interaction (Cases, 1979). The displacement of the adsorption isotherms towards the right as the final outgassing temperature is increased to >100°C may be due to a lowering of the "normal" interaction. This assumption is confirmed, in the same way, by the strong decrease observed in the value of the BET energetical constant C (cf. Table 1, last column).

Finally, the ratio (V_B) argon/(V_B) nitrogen (which is given in the last column of Table 2 and which is only slightly above the minimum ratio of 0.81), the ratio found in a fully microporous sample (Rouguerol *et al.*, 1984), confirms the major role of microporosity in adsorption up to point B. If this ratio is close to the ratio of the molar volumes of the two adsorbates ob-

https://doi.org/10.1346/CCMN.1988.0360304 Published online by Cambridge University Press

tained from the density in the liquid state, nitrogen does not strongly interact with the wall of the channels.

SUMMARY AND CONCLUSIONS

The present study determined the "external" specific surface area of the fibers of sepiolite from Vallecas, Spain, and detected two types of microporosity. Structural microporosity, due to the staggered arrangement of talc ribbons in the fibers, was partly available to N_2 (20%) or CO_2 (52%) molecules and amounted (from the structure parameters) to about 0.25 cm^3/g. Interfiber microporosity was at most equal to 0.03 cm^3/g in the commercial product. The structural microporosity may have been completely eliminated by outgassing at >350°C under conditions of reciprocal thermal analysis. This structural modification (i.e., tilted silicate layers) occurred simultaneously with sintering. The water adsorption isotherms suggested sharp decrease in adsorption energy for outgassing temperatures of >100°C. On the external surface of the fibers, between 3.5 and 2.5 monolayers of water were influenced by the surface field.

ACKNOWLEDGMENTS

This research was supported by D.G.R.S.T grant 81.D.1109 (French Ministry of Industry). The authors are grateful to J. J. Fripiat for numerous discussions. Tolsa S.A. (Spain) kindly supplied the commercial sample of pure sepiolite.

REFERENCES

Anonymous (1976) *Gas Encyclopedia:* L'Air Liquide, ed., Elsevier, Amsterdam, 1150 pp.

Barrer, R. M. and Mackenzie, N. (1954) Sorption by attapulgite. I. Availability of intracrystalline channels: *J. Phys. Chem.* **58,** 560–568.

Barrer, R. M., Mackenzie, N., and MacLeod, D. M. (1959) Sorption of attapulgite. II. Selectivity shown by attapulgite, sepiolite and montmorillonite for n paraffin: *J. Phys. Chem.* **58,** 568–573.

Brauner, K. and Preisinger, A. (1956) Struktur und Entstehung des Sepioliths: *Tschermarks Miner. Petr. Mitt.* **6,** 120–140.

Brindley, G. W. (1959) X-ray and electron diffraction data for sepiolite: *Amer. Mineral.* **44,** 495–500.

Cases, J. M. (1979) Adsorption des tensio-actifs à l'interface solide-liquide: Thermodynamique et influence de l'hétérogénéité des adsorbants: *Bull. Minéral.* **102,** 684–707.

Cases, J. M. and François, M. (1982) Etude des propriétés de l'eau au voisinage des interfaces: *Agronomie* **2,** 931–938.

Dandy, A. J. (1968) Sorption of vapors by sepiolite: *J. Phys. Chem.* **72,** 334–339.

Dandy, A. J. (1971) Zeolitic water content and adsorptive capacity for ammonia of microporous sepiolite: *J. Chem. Soc. A,* 2383–2387.

Dandy, A. J. and Nadiye-Tabbiruka, M. S. (1975) The effect of heating in vacuo on the microporosity of sepiolite: *Clays & Clay Minerals* **23,** 428–430.

De Boer, J. H., Lippens, B. C., Linsen, B. G., Broekhoff, J. C. P., Van den Heuwal, A., and Osinga, Th. J. (1966) The t curve of multimolecular N_2 adsorption: *J. Colloid Interface Sci.* **21,** 405–414.

Delon, J. F. and Cases, J. M. (1970) La mesure de la porosité d'adsorbants à canaux de diamètre constant à partir des isothermes d'adsorption de gaz: *J. Chimie Physique* **no. 4,** 662–666.

Dubinin, M. M. (1966) Modern state of the theory of gas and vapor adsorption by microporous adsorbents: *Pure Appl. Chem.* **10,** 309–321.

Emmett, P. H. and Brunauer, J. (1937) The use of low temperature van der Waals adsorption isotherms in determining the surface area by ion synthetic ammonia catalyst: *J. Amer. Chem. Soc.* **59,** 1553–1564.

Fernandez Alvarez, T. (1970) Superficie especifica y estructura de poro de la sepiolita calentada a diferentes temperaturas: in *Compte-Rendu de la Réunion Hispano-Belga de Minerales de la Arcilla:* J. M. Serratosa, ed., Consejo Superior de Investigaciones Cientificas, Madrid, 202–209.

Fernandez Alvarez, T. (1978) Effecto de la deshidratacion sobre las propriedades adsorbentes de la palygorskita y sepiolita. I. Adsorcion di nitrogeno: *Clay Miner.* **13,** 325–335.

Fripiat, J. J., Cases, J. M., François, M., and Letellier, M. (1982) Thermodynamic and microdynamic behavior of water in clay suspensions and gels: *J. Colloid Interface Sci.* **89,** 378–400.

Fripiat, J. J., Letellier, M., and Levitz, P. (1984) Interaction of water with clay surfaces: *Phil. Trans. R. Soc. London, A* **311,** 287–289.

Guérin, H., Siemieniewska, T., Grillet, Y., and François, M. (1970) Influence de la chimisorption d'oxygène sur la détermination de l'oxyréactivité des combustibles solides. I. Etude du semi coke de lignite préparé à 550°C: *Carbon* **8,** 727–740.

Hagymassy, J., Brunauer, S., and Mikhail, R. Sh. (1969) Pore structure analysis by water vapor adsorption. I. t curves for water vapor: *J. Colloid Interface Sci.* **29,** 485–491.

Harkins, W. D. and Jura, G. (1944) An absolute method for the determination of the area of a finely divided crystalline solid: *J. Amer. Chem. Soc.* **66,** 1362–1365.

Jiménez-Lopez, A., de López-Gonzáles, D., Ramirez-Säenz, A., Rodriguez-Reinoso, F., Valenzuela-Colahorro, C., and Zurita-Herrera, L. (1978) Evolution of surface area in a sepiolite as a function of acid and heat treatment: *Clay Miner.* **13,** 375–385.

Lippens, B. C. and de Boer, J. H. (1965) Studies on pore systems in catalysts. V. The t method: *J. Catalysis* **4,** 319–323.

McClellan, A. L. and Harnsberger, H. F. (1967) Cross sectional areas of molecules adsorbed on solid surfaces: *J. Colloid Interface Sci.* **23,** 577–599.

Mikhail, R. Sh., Brunauer, S., and Bodor, E. E. (1968) Investigation of a complete pore structure analysis. I. Analysis of micropores: *J. Colloid Interface Sci.* **26,** 43–53.

Moller, K. P. and Kolterman, M. (1965) Gas Adsorption und Struktur von Sepiolit: *Z. Anorg. Allg. Chem.* **41,** 36–40.

Nagy, B. and Bradley, W. F. (1955) The structural scheme of sepiolite: *Amer. Mineral.* **40,** 885–892.

Partyka, S., Rouquerol, F., and Rouquerol, J. (1979) Calorimetric determination of surface areas. Possibilities of a modified Harkins and Jura procedure: *J. Colloid Interface Sci.* **68,** 21–31.

Pauling, L. (1940) *The Nature of the Chemical Bond:* Cornell Univ. Press, Ithaca, New York, 450 pp.

Preisinger, A. (1963) Sepiolite and related compounds. Its stability and applications: in *Clays and Clay Minerals, Proc. 10th Natl. Conf., Austin, Texas, 1961,* Ada Swineford and P. C. Franks, eds., Pergamon Press, New York, 365–371.

Prost, R. (1975) Etude de l'hydratation des argiles. Interactions eau-minéral et mécanisme de la rétention de l'eau: *Ann. Agron.* **26,** 401–461.

Rautureau, M. and Mifsud, A. (1977) Etude par microscopie électronique des différents états d'hydratation de la sépiolite: *Clay Miner.* **12,** 309–318.

Rautureau, M. and Tchoubar, C. (1976) Structural analysis of sepiolite by selected area electron diffraction. Relations with physicochemical properties: *Clays & Clay Minerals* **24,** 43–49.

Rouquerol, J. (1970) L'analyse thermique à vitesse de décomposition constante: *J. Thermal Analysis* **2,** 123–140.

Rouquerol, J. (1972) *Calorimétrie d'Adsorption aux Basses Températures. I. Thermochimie:* CNRS Pub., Paris, 538 pp.

Rouquerol, J. (1987) Reciprocal thermal analysis. The hidden face of thermal analysis: *Thermochimica Acta* (in press).

Rouquerol, J. and Davy L. (1978) Automatic gravimetric apparatus for recording adsorption isotherms of gases or vapours onto solids: *Thermodynamica Acta* **24,** 391–397.

Rouquerol, J., Rouquerol, F., Grillet, Y., and Torralvo, M. J. (1984) Influence of the orientation of the nitrogen molecule upon its actual cross-sectional area in the adsorbed monolayer: in *Fundamentals of Adsorption,* A. L. Myers and G. Belfort, eds., Engineering Foundation, New York, 501–512.

Sing, K. S. W. (1967) Assessment of microporosity: *Chemistry and Industry,* 829–830.

Sing, K. S. W., Everett, D. H., Haul, R. A. W., Moscou, L., Pierotti, R. A., Rouguerol, J., and Siemieniewska, T. (1985) Reporting physisorption data for gas/solid systems. IUPAC recommendation: *Pure Appl. Chem.* **57,** 603–619.

(Received 16 May 1987; accepted 2 November 1987; Ms. 1673)